Journal of Pharmaceutical & Biomedical Analysis
Vol. 7, No. 12, pp. 1599–1610, 1989
Printed in Great Britain

0731–7085/89 $3.00 + 0.00
Pergamon Press plc

Structural characterization of cisplatin analogues by fast atom bombardment (FAB) and laser microprobe mass spectrometry (LAMMA)*

J. CLAEREBOUDT,† B. DE SPIEGELEER,‡ E. A. DE BRUIJN,§ R. GIJBELS‖ and M. CLAEYS†¶

† *Department of Pharmaceutical Sciences, University of Antwerp (U.I.A.), Universiteitsplein 1, B-2610 Wilrijk, Belgium*
‡ *Laboratory of Pharmaceutical Chemistry and Pharmaceutical Analysis, State University of Gent, Harelbekestraat 72, B-9000 Gent, Belgium*
§ *Department of Medicine, University of Antwerp (U.I.A.), Universiteitsplein 1, B-2610 Wilrijk, Belgium*
‖ *Department of Chemistry, University of Antwerp (U.I.A.), Universiteitsplein 1, B-2610 Wilrijk, Belgium*

Abstract: The present study is concerned with the investigation of the potentials and limitations of fast atom bombardment (FAB) and laser microprobe mass spectrometry (LAMMA) for the structural characterization of a series of cisplatin analogues. The limiting factors for obtaining good quality FAB spectra are the solubility and the stability of the organometallic platinum complexes in the FAB matrix. In the case of a suitable matrix being found, molecular weight information is derived from the $(M + H)^+$ and/or $(M - H)^-$ ions. Drawbacks of the application of FAB are (i) the low signal intensities of the molecular ion-like species as compared to the matrix signals and (ii) the scarcity of fragmentation necessary for structure determination. Combination of FAB with tandem mass spectrometry was used to overcome these problems. LAMMA provides a valuable alternative for the direct mass spectral analysis of cisplatin analogues. For some compounds, LAMMA results in useful mass spectra, whereas FAB fails. The abundant fragmentation yields structural information which is complementary for positive and negative ions. The laser power density applied to the sample is of critical importance for the quality of the spectra.

Keywords: *Cisplatin analogues; platinum complexes; mass spectrometry; laser microprobe mass analysis (LAMMA); fast atom bombardment (FAB).*

Introduction

Rosenberg's discovery of the antitumour activity of *cis*-$Pt(NH_3)_2Cl_2$ (cisplatin) stimulated considerable interest in the chemistry and pharmacology of this and other structurally related complexes of platinum [1–4]. Cisplatin has become one of the most

*Presented at the "Third International Symposium on Drug Analysis", May 1989, Antwerp, Belgium.
¶To whom correspondence should be addressed.

extensively used of all antitumour drugs and has been applied with major success in the treatment of various types of solid tumours. Monitoring and characterization of cisplatin and its biologically important metabolites in body fluids (plasma and urine) is very important for the study of its mode of action and for the optimalization of the chemotherapy. A variety of commonly used analytical procedures for the determination of cisplatin and its analogues have been reviewed by Riley [5].

One challenge to the chemist is to search for suitable "structural information-rich" methods that are applicable to this class of compounds and that can be applied to very small (microgram or less) quantities. To this end, we have investigated the potentials of mass spectrometry. Due to their non-volatility and thermal instability, the platinum containing organometallic complexes are difficult to study by conventional mass spectrometry: nearly all attempts at volatilization from a direct probe, completely degraded the complexes, except for cisplatin. As a consequence, only very few mass spectral data for this class of compound are available in the literature [6–14]. The aim of this paper is to evaluate the potentials and limitations of FAB–MS and LAMMA, as alternatives to conventional mass spectrometry, for the analysis of a series of cisplatin analogues (Fig. 1). Attention will be focussed on the complementary character of these two desorption ionization (DI) techniques, with respect to sample requirements, structural information (i.e. molecular weight vs fragments) and analytical applicability.

Experimental

Mass spectrometry

FAB and electron impact (EI) analysis were performed on a VG 70-SEQ hybrid mass spectrometer (VG Analytical Ltd, Manchester, UK). The Instrument consists of a high-

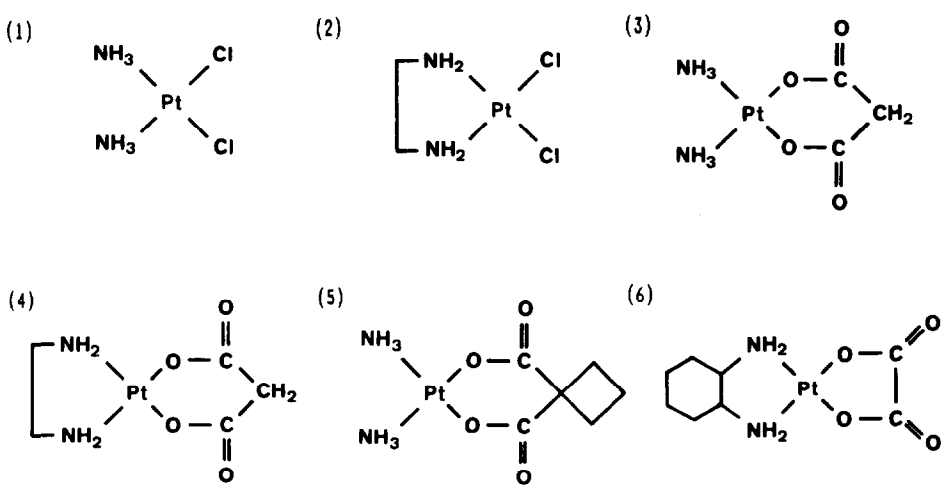

Figure 1
Structures of the platinum(II) complexes studied. Number, name, type of complex (L_A = bidentate diamine ligand, L_B = bidentate dicarboxylate ligand): (**1**) *cis*-dichlorodiammineplatinum(II): *cis*-$Pt(NH_3)_2Cl_2$ (cisplatin); (**2**) *cis*-dichloroethylenediamineplatinum(II): PtL_ACl_2; (**3**) diammine(malonato)platinum(II): $Pt(NH_3)_2L_B$; (**4**) ethylenediamine(malonato)platinum(II): PtL_AL_B; (**5**) diammine(1,1-cyclobutanedicarboxylato)platinum(II): $Pt(NH_3)_2L_B$ (Carboplatin); (**6**) 1*R*,2*R*-diaminecyclohexane (oxalato)platinum(II): PtL_AL_B.

resolution double-focussing mass spectrometer with EB configuration (MS–I) followed by an RF-only quadrupole collision gas cell and a high performance quadrupole mass analyser (MS–II). Mass spectra were recorded under control of the VG 11-250J data system by repetitive scanning of MS–I over the range 20–500 a.m.u., using a scan time of 2 s decade^{-1}. Daughter ion spectra were obtained by collisionally activated decomposition (CAD) in the third field-free region (RF-only quadrupole gas cell), using argon as collision gas, and by scanning MS–II. For EI–MS, samples were introduced with the direct inlet probe, which was gradually heated from 50 to 300°C, and ionized with a 70 eV electron beam. In FAB, the samples were dissolved in a matrix, loaded on a stainless steel FAB probe tip and ionized with 8 keV xenon atoms.

Laser microprobe mass spectra were obtained using a LAMMA®-500 instrument (Leybold–Heraeus, Köln, FRG) which has been described elsewhere [15]. The output of a Q-switched Nd–YAG pulsed laser (λ = 265 nm, 15 ns pulse width) was focussed on the sample with a microscope objective. The laser power could be varied by using a continuously variable, neutral optical density filter. Unless otherwise reported, the laser power was attenuated to keep the laser irradiation close to the ion formation threshold (i.e. 10^7–10^8 W cm^{-2}). All samples (powders) were supported by Formvar coated TEM-grids and particles of approximately 1 μm diameter were selected for analysis. Additional information on the experimental protocol for organic analysis with the LAMMA-500 is reported in the literature [16]. One of the major disadvantages of the LAMMA instrumentation is the limited mass resolution (M/ΔM = 600), which does not allow the exact mass measurement of the detected ions. Therefore, the proposed structural assignments and fragmentation patterns should be regarded as tentative.

Materials

Figure 1 lists all the investigated cisplatin analogues (**1–6**) with their name, structure and complex type. These compounds were synthesized by the method described by Dhara [17], which is characterized by the iodoplatinum intermediate [18]. UV, IR, HPTLC and HPLC co-elution with reference compounds were used to confirm the purity and identity of the synthesized complexes [19]. The FAB matrices (i.e. glycerol, thioglycerol and *m*-nitrobenzylalcohol) and all other organic solvents used were purchased from Janssen Chimica (Belgium).

Results and Discussion

Electron impact (EI)

In contrast to the other platinum complexes (**2–6**), cisplatin **1** does not undergo complete thermal degradation during heating on a solid probe and therefore, a useful EI spectrum (70 eV) could be obtained (Fig. 2). Ions containing platinum or platinum as well as chlorines are readily recognized by their characteristic isotopic distribution listed in Table 1. The *m/z* values listed in the text correspond to the cluster ions containing only the ^{194}Pt and ^{35}Cl isotopes. Together with the molecular ion $[Pt(NH_3)_2Cl_2]^{+\cdot}$ at *m/z* 298, the following fragments are observed: $[Pt(NH_3)Cl_2]^{+\cdot}$ (*m/z* 281), $[Pt(NH_3)(NH_2)Cl]^{+\cdot}$ (*m/z* 262), $[Pt(NH_2)Cl]^{+\cdot}$ (*m/z* 245), $[Pt(NH_3)_2]^{+\cdot}$ (*m/z* 228), $[Pt(NH_2)]^{+}$ (*m/z* 210) and $Pt^{+\cdot}$ (*m/z* 194). Deviations from the theoretical distributions for these ions indicate that less abundant fragment ions {i.e. $[Pt(NH_3)_2Cl]^{+}$ (*m/z* 263), $[Pt(NH_3)Cl]^{+}$ (*m/z* 246), $(PtCl)^{+}$ (*m/z* 229) and $[Pt(NH_3)]^{+\cdot}$ (*m/z* 211)} are also formed.

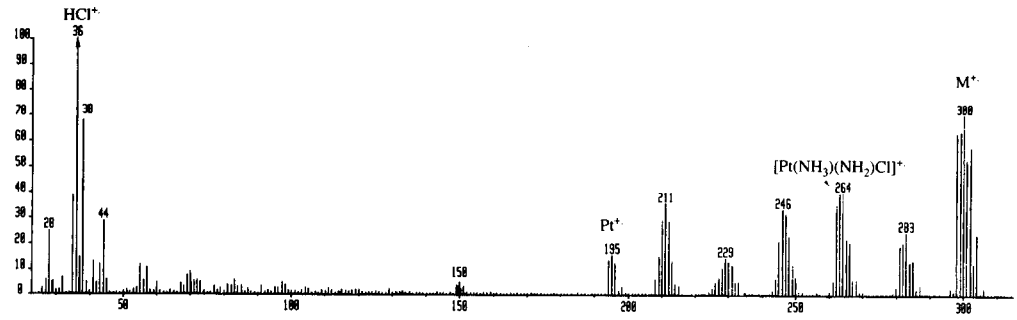

Figure 2
Positive ion EI spectrum of cisplatin (**1**).

Table 1
Theoretical isotopic distribution for ionic species containing platinum and chlorine

	(A − 2)	A*	(A + 1)	(A + 2)	(A + 3)	(A + 4)	(A + 5)	(A + 6)	(A + 7)	(A + 8)
Pt	2	97	100	75	0	21				
PtCl	2	93	94	100	30	43	0	6		
$PtCl_2$	2	72	73	100	47	58	7	15	0	2
$PtCl_3$	1	59	59	100	57	73	18	28	2	5

*A corresponds with the isotope ^{194}Pt.

Fast atom bombardment (FAB)

In general, the quality of the FAB spectra is dependent on the solubility of the neutral platinum(II) complexes in the matrix. Therefore, different FAB matrices such as glycerol, thioglycerol, magic bullet, *m*-nitrobenzylalcohol (*m*-NBA), triethanolamine and 18-crown-6 with 10% tetraglyme, were tested. Compounds **5** and **6** were successfully analysed in pure glycerol or *m*-NBA. For complexes **1–4**, the matrices mentioned above, failed to produce useful FAB spectra. To improve the solubility of these compounds, dimethylsulphoxide (DMSO) was added as a co-solvent. With a mixed solvent system of DMSO and glycerol (1:3, v/v) the chlorine containing complexes were readily dissolved and a slight improvement in solubility was obtained for products **3** and **4**. The same effect was observed with a DMSO–*m*-NBA (1:3) and a DMSO–thioglycerol (1:3) mixture.

Despite the efforts to find a suitable matrix for each compound, we were not successful in desorbing diammine(malonato)platinum (**3**) by FAB. Diagnostic ions observed in the positive and negative ion FAB spectra of the other complexes are summarized in Table 2. As an example, the positive and negative ion FAB spectrum of ethylenediamine (malonato)platinum **4** is illustrated in Fig. 3a, b. The results obtained for compounds **4–6** indicate that FAB mainly yields molecular mass information, derived from the $(M + H)^+$ and $(M - H)^-$ ions and related adduct ions {i.e. $(M + H + Gly)^+$, $(M - H + Gly)^-$ and $[M + (L_B + H)]^-$}. With the exception of the $(M - H - NH_3)^-$ fragment of carboplatin **5** no platinum containing fragment ions are observed in the spectra. The $(L_A + H)^+$ and $(L_B + H)^-$ ions, which are related to the bidentate diamine and dicarboxylate ligands, are the only structurally relevant fragment ions available. Formation of the $(L_B + H)^-$ ion implies that a proton transfer from the L_A ligand to the L_B ligand occurs (*vide infra*: LAMMA results). Problems can arise when

Table 2
Positive and negative ion FAB data for cisplatin analogues **1–6**

Structure number		[1]		[2]
Molecular weight*		298		324
Matrix†		DMSO–Glyc		DMSO–Glyc
Positive ion FAB data*,§,‖				
$(M - Cl + DMSO + Gly)^+$		433 (W)		459 (VW)
$(M - Cl + 2\ DMSO)^+$		419 (VW)		445 (W)
$(M + H + Gly)^+$		391 (M)		417 (VW)
$(M + H + DMSO)^+$		377 (W)		403 (M)
$(M - Cl + DMSO)^+$		341 (S)		367 (S)
$(M + H)^+$				
$(L_A + H)^+$				61 (M)
Negative ion FAB data*,§,‖				
$(M - H + Gly)^-$		389 (VW)		415 (VW)
$(M - H)^-$		297 (W)		323 (W)
Cl^-		35 (M)		35 (M)
Structure number	[3]	[4]	[5]	[6]
Molecular weight*	330	356	370	396
Matrix†	No‡	DMSO–Glyc	Glyc	Glyc
Positive ion FAB data*,§,‖				
$(M + H + Gly)^+$		449 (VW)	463 (W)	489 (VW)
$(M + Na)^+$			393 (VW)	
$(M + H)^+$		357 (W)	371 (S)	397 (M)
$(L_A + H)^+$		61 (M)		115 (M)
Negative ion FAB data*,§,‖				
$(M + (L_B + H))^-$		459 (VW)	513 (W)	
$(M - H + Gly)^-$		447 (VW)		487 (VW)
$(M - H)^-$		355 (W)	369 (W)	395 (W)
$(M - H - NH_3)^-$			352 (W)	
$(L_B + H)^-$		103 (M)	143 (M)	

*Molecular weight and ion masses referenced to the isotopes ^{194}Pt and ^{35}Cl.
†Glyc = glycerol; DMSO–Glyc = mixed solvent system (1:3, v/v).
‡No suitable matrix was found for diammine(malonato)platinum(II) **3**.
§Relative ion abundances: VS = very intense (S/N > 50), S = intense (S/N 30–50), M = moderately intense (S/N 10–30), W = weak (S/N 5–10), VW = very weak (S/N 3–5).
‖L_A = bidentale with diamine structure; L_B = bidentate ligand with dicarboxylate structure.

low mass fragment ions are obscured by ions originating from the matrix. For example, this is the case for the $(L_A + H)^+$ ion (*m/z* 61) of compound **4** which overlaps with the $(Gly + H - CH_3OH)^+$ ion (*m/z* 61) of glycerol.

For the cisplatin analogues containing chlorine ligands, **1**, **2**, the observed ions indicate that condensed phase chemical reactions occur between the platinum complexes and the DMSO–glycerol matrix, when the sample is exposed to the fast atom beam. The two mechanisms causing the ionization can be explained by the exchange of a chlorine ligand with DMSO, yielding an intense $(M - Cl + DMSO)^+$ ion signal and adduct formation of the cisplatin analogues with the ionized solvents, giving rise to ions such as $[M + (Gly + H)]^+$, $[M + (DMSO + H)]^+$ and $[M + (Gly - H)]^-$. For a detailed discussion of these solute–matrix interactions, reference is made to the work of Siegel *et*

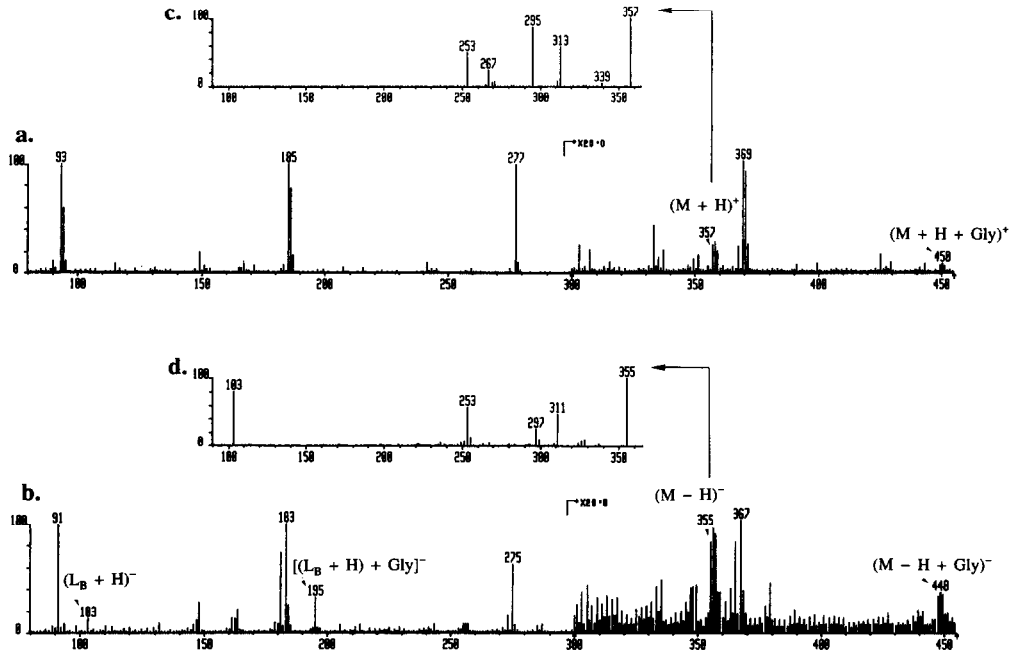

Figure 3
FAB mass spectra of ethylenediamine(malonato)platinum(II) **4** (matrix = DMSO–glycerol): (a) positive and (b) negative ion mode. Background ions are unlabelled. Daughter ion spectra of $(M + H)^+$ (*m/z* 357) (c) and $(M - H)^-$ (*m/z* 355) (d) obtained by CAD at collision energy of 25 eV and using an argon gas pressure of 2 mtorr.

al. [13], who observed the same type of ions for a series PtL_ACl_2 compounds analysed in a mixed DMSO–thioglycerol matrix.

From the results obtained for cisplatin analogues **1–6**, we can conclude that FAB mainly yields molecular weight information and that the major drawbacks of the technique for the analysis of these neutral platinum(II) complexes are related to (i) the low solubility and the instability of the complexes in the FAB matrix, (ii) the lack of diagnostic Pt-containing fragment ions which are necessary for structural characterization, (iii) the low signal intensities of the molecular ion-like species as compared to the matrix signals and (iv) the presence of interfering background ions originating from the matrix and other sample constituents.

Tandem mass spectrometry (MS/MS) with collisionally activated decomposition (CAD) is a technique, which, when combined with FAB, can overcome some of these drawbacks. As an example, the CAD spectra of the $(M + H)^+$ (*m/z* 357) and $(M - H)^-$ ions (*m/z* 355) of ethylenediamine(malonato)platinum **4**, are shown in Fig. 3c, d. The $(M + H)^+$ ion (*m/z* 357) decomposes by the loss of even electron species giving rise to the fragments at *m/z* 339 (loss of H_2O), *m/z* 313 (loss of CO_2), *m/z* 311 (loss of HCOOH), *m/z* 295 (combined loss of H_2O and CO_2), *m/z* 267 (combined loss of CO_2 and HCOOH) and *m/z* 253 [loss of $(L_B + 2H)$]. The loss of neutral molecules such as CO_2 and the dicarboxylic acid $(L_B + 2H)$ from the $(M + H)^+$ ion is also observed in the CAD spectra of compounds **5** and **6** and seems to be characteristic for the platinum complexes containing a bidentate dicarboxylate ligand (L_B). The CAD spectrum of the

$(M - H)^-$ ion (*m/z* 355) is dominated by the malonate anion $(L_B + H)^-$ at *m/z* 103. Formation of the $(L_B + H)^-$ ion from the $(M - H)^-$ is typical for the complexes containing a bidentate dicarboxylate ligand, **4–6**. The ion at *m/z* 297 is formed by the expulsion of the $(L_A - 2H)$ moiety. This was also observed for compounds **2** and **6** and thus seems to be characteristic for the complexes containing a bidentate diamine ligand (L_A). The other fragments in the CAD spectrum of $(M - H)^-$ result from the expulsion of CO_2 (*m/z* 311) and of $(L_A - 2H)$ and CO_2 (*m/z* 253). This example illustrates that the CAD spectra of the $(M + H)^+$ and $(M - H)^-$ ions, desorbed by FAB, provide a wealth of structurally relevant fragment ions, enabling us to characterize the structure of the investigated complex. A detailed report about the potentials of the FAB/MS/CAD/MS technique for the structural characterization of cisplatin analogues and adducts with nucleobases has been published elsewhere [14].

Laser microprobe mass analysis (LAMMA)

The discussion will be confined to the LAMMA results obtained for compounds **1**, **3** and **6**, which correspond to three different types of cisplatin analogues. These examples will allow us (i) to illustrate the potentials of the laser microprobe as an alternative to FAB, (ii) to study the fragmentation pathways induced by laser impact and (iii) to check the influence of the laser energy density on the quality of the spectra.

Laser microprobe analysis does not make use of a liquid matrix and, therefore, in contrast to FAB (see Table 2), solute–matrix reactions are not observed for cisplatin, **1**. The positive ion LAMMA spectrum of cisplatin (**1**) contains the molecular ion $[Pt(NH_3)_2Cl_2]^{+\cdot}$ at *m/z* 298 (Fig. 4a). Sequential loss of the ligands leads to the detection of $[Pt(NH_3)_2Cl]^+$ (*m/z* 263), $[Pt(NH_3)Cl]^+$ (*m/z* 246), $[Pt(NH_3)_2]^{+\cdot}$ (*m/z* 228),

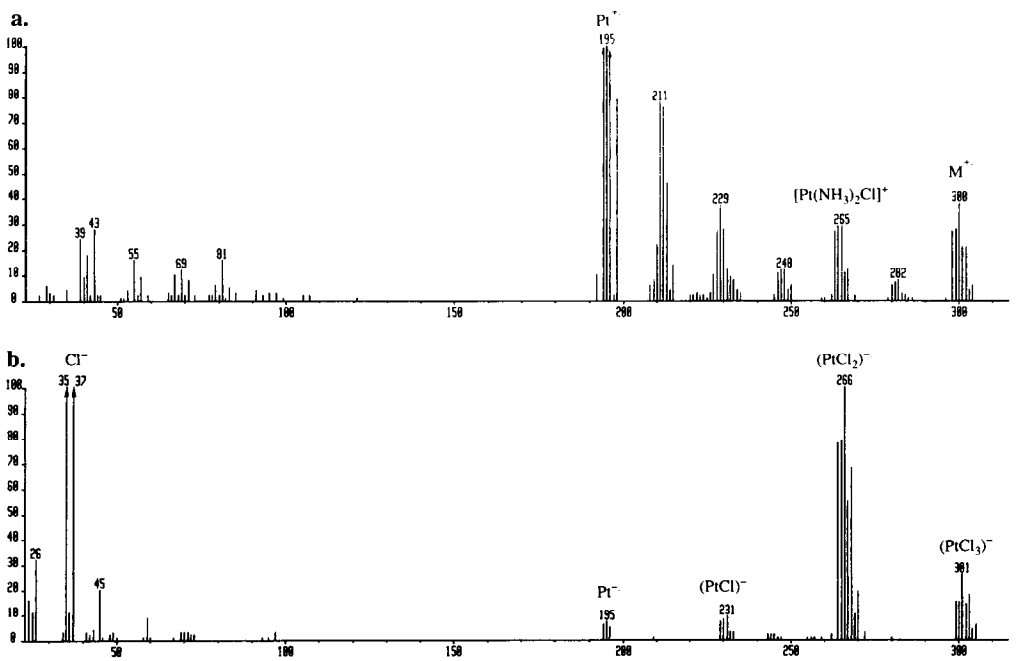

Figure 4
LAMMA mass spectra of cisplatin (**1**): (a) positive and (b) negative ion mode.

$[Pt(NH_3)]^{+\cdot}$ (*m/z* 211), and $Pt^{+\cdot}$ (*m/z* 194). Less abundant fragment ions are present at *m/z* 281 $[Pt(NH_3)Cl_2]^{+\cdot}$, *m/z* 280 $[Pt(NH_2)Cl_2]^{+}$, *m/z* 229 $(PtCl)^{+}$, *m/z* 227 $[Pt(NH_3)(NH_2)]^{+}$ and *m/z* 210 $[Pt(NH_2)]^{+}$. Two binuclear platinum cluster ions $(Pt_2)^{+\cdot}$ (*m/z* 388) and $(Pt_2N)^{+}$ (*m/z* 402) are detected with low abundance in the high mass region. The occurrence of the odd-electron molecular ion (*m/z* 298) and the extensive fragmentation makes it of interest to compare the LAMMA spectrum with the EI spectrum of cisplatin (Fig. 2). In the LAMMA spectrum, the higher degree of fragmentation and the preferential loss of chlorine radical(s) (i.e. cleavage processes) can be noticed, whereas in EI, rearrangement type processes (e.g. loss of NH_3 and/or HCl) prevail. These observations indicate that the amount of internal energy, imparted to the molecular ion as vibrational energy is larger for laser impact than for electron ionization at 70 eV. These results are in agreement with earlier studies which demonstrated that LAMMA cannot be considered as a real "soft" desorption ionization technique [20, 21]. We reiterate that the LAMMA spectrum was obtained at threshold (minimum) laser energy. Using higher laser energies results in an increase of the elemental Pt^{+} signal at the cost of the signal intensities for the parent ion and structurally informative fragment ions.

In the negative ion LAMMA spectrum of cisplatin (Fig. 4b), the only platinum-containing ions observed can be attributed to $(PtCl_n)^{-}$, where $n = 0$–4. Apparently, no amine groups are retained in the negative ions formed. The presence of the ions $Pt^{-\cdot}$ (*m/z* 194), $(PtCl_3)^{-}$ (*m/z* 299) and $(PtCl_4)^{-\cdot}$ (*m/z* 334) should be noted. The abundance of the $Pt^{-\cdot}$ ion suggest that an energetically favoured process is involved, which can be defined as the complete filling-up of the 5*d*-orbitals of platinum. Formation of the $(PtCl_3)^{-}$ and $(PtCl_4)^{-\cdot}$ ions can be rationalized by recombination reactions between neutral and ionized fragments of cisplatin, occurring in the laser induced microplasma. In the lower mass range the chlorine anion (*m/z* 35) is detected.

The LAMMA spectra obtained for 1*R*,2*R*-diaminecyclohexane(oxalato)platinum **6**, a cisplatin analogue of the PtL_AL_B class, represents a good example to illustrate the complementary nature of the structural information gained from positive and negative ions (Fig. 5). In the positive ion mode, molecular weight information is derived from the $(M + H)^{+}$ (*m/z* 397) and $(M + Na)^{+}$ (*m/z* 419) ions. The presence of $(L_A + H)^{+}$ (*m/z* 115) and $(L_A + Na)^{+}$ (*m/z* 137) ions indicate that protonation and cationization take place on the diamine ligand (L_A). The ion at *m/z* 307 corresponds to $[Pt(L_A - H)]^{+}$. Subsequent consecutive losses of H_2 molecules yield (conjugated) fragments at *m/z* 305, 303, 301 and 299. The ions at *m/z* 288 and 286 can be explained by combined expulsion of NH_3 and one or two H_2 molecules, respectively. The majority of the fragments in the *m/z* 200–280 mass range correspond to $(PtNC_nH_m)^{+}$ type ions. Unequivocal interpretation, however, is hindered by the low abundance and the overlapping isotopic clusters of these ions. The high signal intensities of the Pt^{+} element ion and of the fragment ions related to L_A ($m/z < 115$) point again to the high internal energy of the molecular species formed by laser impact.

The negative ion LAMMA spectrum gives information about the remaining part of the complex [i.e. the oxalate ligand (L_B)]. In the high mass region a characteristic $[Pt(L_B + H)]^{-}$ fragment ion is detected at *m/z* 283. Expulsion of CO_2 or CO_2 and CO from this ion leads to the fragments at *m/z* 239 and 211, respectively. The base peak at *m/z* 89 corresponds to the $(L_B + H)^{-}$ ion and related fragments are present at *m/z* 61 $(HOCO_2^{-})$ and *m/z* 45 (HCO_2^{-}). The presence of a $(L_B + H)^{-}$ anion appears to be typical for all the cisplatin analogues which contain a bidentate dicarboxylate ligand (L_B) (i.e. compounds **3**–**6**). The remaining signals in the spectrum correspond to CN^{-} (*m/z*

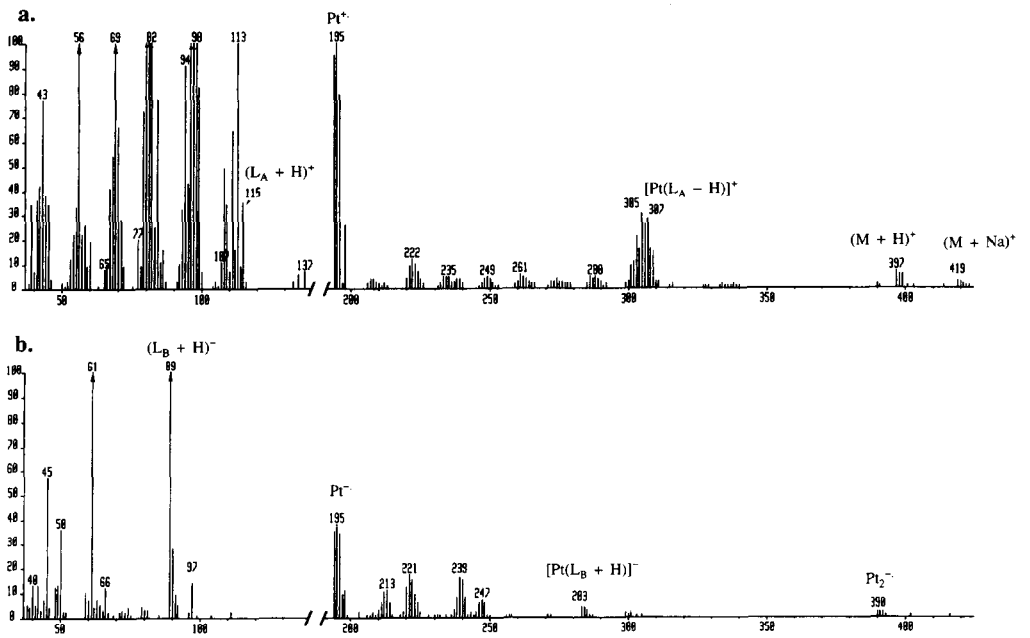

Figure 5
LAMMA mass spectra of 1*R*,2*R*-diaminecyclohexane(oxalato)platinum(II) (**6**): (a) positive and (b) negative ion mode.

26), C_3N^- (*m/z* 50), $Pt^{-\cdot}$ (*m/z* 194) and some non-specific platinum-containing clusters {i.e. $[Pt(CN)]^-$ (*m/z* 220), $[Pt(CO_2)]^{-\cdot}$ (*m/z* 238) and $[Pt(CN)_2]^{-\cdot}$ (*m/z* 246)}.

The formation of fragment ions such as $(L_B + H)^-$ and $[Pt(L_B + H)]^-$ in the negative ion mode and $[Pt(L_A - H)]^+$ in the positive spectrum implies that a proton is transferred from the diamine (L_A) to the oxalate (L_B) ligand, whereby the L_A ligand becomes covalently bonded to the platinum. A mechanism is proposed in Scheme 1. Proton transfer from the (di)amine ligand to the dicarboxylate ligand seems to be a general step in the fragmentation of PtL_AL_B and $Pt(NH_3)_2L_B$ type complexes. This process was also reported for the FAB MS/MS experiments, where fragmentation was induced by CAD [14].

As neither EI nor FAB provide useful mass spectra for diammine(malonato)platinum **3** (Table 2), it was of interest to check whether LAMMA results in structurally informative mass spectra. In the positive ion spectrum, molecular weight information can be derived from the protonated $(M + H)^+$ (*m/z* 331) and cationized $(M + Na)^+$ (*m/z* 353) species (Fig. 6a). The fragment ions $[Pt(NH_3)_2]^{+\cdot}$ (*m/z* 228), $[Pt(NH_3)]^{+\cdot}$ (*m/z* 211) and $Pt^{+\cdot}$ (*m/z* 194) are formed by loss of the intact ligands, L_B, L_B and NH_3, L_B and 2

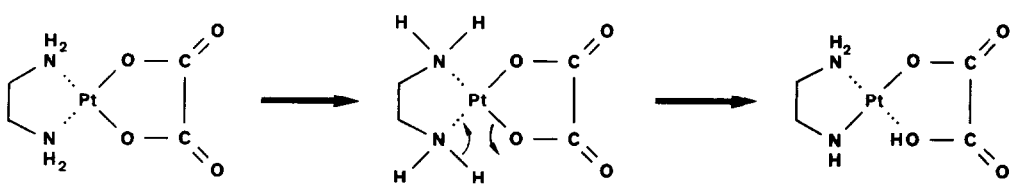

Scheme 1.

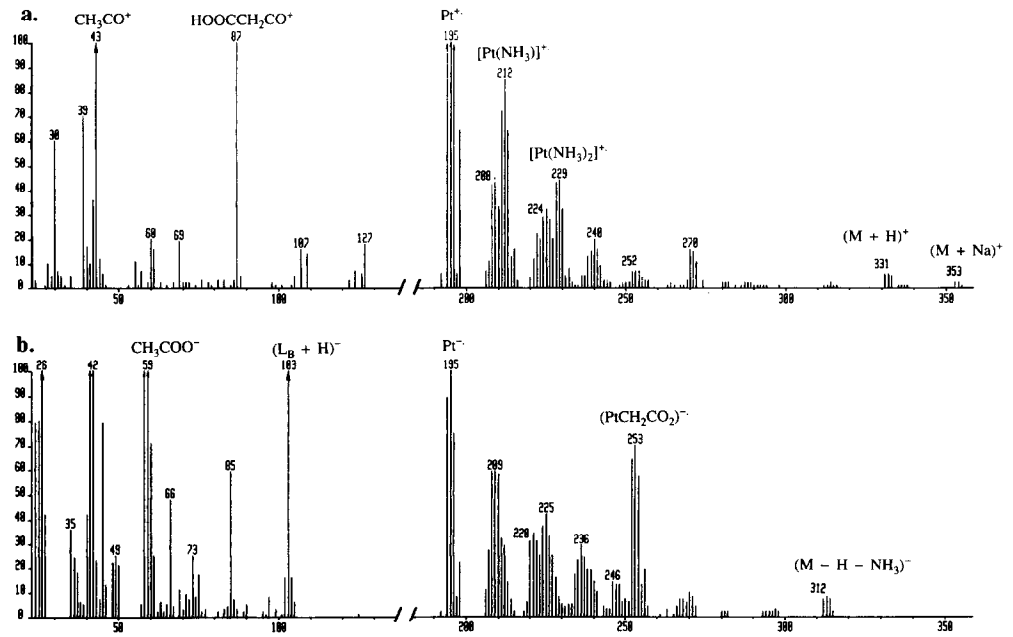

Figure 6
LAMMA mass spectra of diammine(malonato)platinum(II) (**3**): (a) positive and (b) negative ion mode.

NH_3, respectively. The odd-electron state of these fragments indicate that they originate from the molecular ion $M^{+\cdot}$, which itself is not detected in the spectrum. Most probably, the high vibrational excitation and the energetically unfavourable odd-electron situation, results in the complete fragmentation of the molecular ion. The other platinum-containing fragment ions are tentatively assigned as $[Pt(NH_3)(OOCCH_3)]^+$ (*m/z* 270), $[Pt(NH_2)(CH_2CO)]^+$ (*m/z* 252), $[Pt(NH_2)(OCH_2)]^+$ (*m/z* 240), $[Pt(CO_2)]^{+\cdot}$ (*m/z* 238) and $[Pt(NH_2)(CH_2)]^+$ (*m/z* 224). The lower mass region of the spectrum contains two abundant fragment ions, $HOOCCH_2CO^+$ (*m/z* 87) and CH_3CO^+ (*m/z* 43), which are related to the malonate ligand. The formation of these ions and the fragment ions containing an amino group, covalently bonded to platinum (see above), probably involves a proton transfer from the amine to the malonate ligand (analogous to compound **6**, Scheme 1). At high mass, the binuclear platinum species $(Pt_2)^{+\cdot}$ (*m/z* 388), $(Pt_2C)^{+\cdot}$ (*m/z* 400) and $(Pt_2N)^+$ (*m/z* 402), are recorded.

The negative ion LAMMA spectrum of diammine(malonato)platinum, **3**, contains a $(M - H - NH_3)^-$ ion at *m/z* 312 (Fig. 6b). This type of ion was also observed for carboplatin **5**. The intense signal at *m/z* 252 can be attributed to the $(PtCH_2CO_2)^{-\cdot}$ fragment. Next to the intense $Pt^{-\cdot}$ signal (*m/z* 194), a series of structurally non-specific, platinum-containing cluster ions is observed (*m/z* 200–250). Most of these ions are formed through gas phase reactions of platinum with small anions (i.e. CN^-, OCN^-, etc.), which are commonly encountered in the negative LAMMA spectra of nitrogen containing organic compounds. In the low *m/z* range, the $(L_B + H)^-$ ion (*m/z* 103) and fragments thereof (*m/z* 85, 59, 58, 45 and 41) are detected. The remaining signals at low mass correspond to less specific recombination type anions [i.e. CN^- (*m/z* 26), OCN^-

(m/z 42), C_3NO^- (m/z 66) and $C_n(H)^-$ (n = 1–4)]. At high mass, the binuclear platinum cluster ions $(Pt_2)^{-\cdot}$, $(Pt_2C)^{-\cdot}$, $(Pt_2N)^-$ and $(Pt_2CN)^-$ are observed.

The results obtained for compound **3** clearly indicate that, in contrast to FAB and EI, LAMMA yields structural information. It is remarkable that the positive ion LAMMA spectrum mainly gives molecular weight information and structural information which points to the presence of two NH_3 ligands, whereas, "complementary" information about the remaining malonate ligand is provided by the negative ion spectrum. All this structural information, however, is lost when a higher laser power is applied, resulting ultimately in the detection of only $Pt^{+/-\cdot}$ elemental ions and non-specific cluster ions {e.g. $(Pt_2)^{+/-\cdot}$, $(Pt_2C)^{+/-\cdot}$ and $[Pt(CN)_n]^-$)}, formed by recombination reactions in the laser induced microplasma.

Conclusion

The applicability of FAB–MS for the structural characterization of cisplatin analogues is limited by the poor solubility and the instability of the complexes in the matrix and the lack of diagnostic fragment ions in the spectra. Structural information could only be obtained by collisionally induced fragmentation of the molecular ion-like species.

LAMMA is a valuable "complementary" technique to FAB–MS. Neutral platinum(II) complexes with low proton affinities, which do not desorb efficiently by FAB and are sparingly soluble or undergo ligand-exchange reactions in the standard FAB matrices, can be studied more readily by LAMMA. Furthermore, the degree of fragmentation is much higher in LAMMA than in FAB, providing structural information which is gained from positive as well as negative ions. Another interesting feature of LAMMA is the extremely small sample consumption (not discussed in this paper), which may represent an asset for biological applications.

Acknowledgements — Financial support for the mass spectrometer by the Belgian National Fund for Medical Research (Grant Nr. 3.0089.87) and the Belgian Government (Grant Nr. 87/92-102) is gratefully acknowledged. M. Claeys is indebted to the National Fund for Scientific Research as a research associate. We also thank H. Van den Heuvel for help in the preparation of this manuscript.

References

[1] B. Rosenberg, L. Van Camp, J. E. Trosko and H. Mansoup, *Nature* **222**, 385 (1969).
[2] T. A. Connors and J. J. Roberts (Eds), *Platinum Coordination Complexes in Cancer Chemotherapy*. Springer-Verlag, Heidelberg (1974).
[3] A. W. Prestayko, S. T. Crooke and S. K. Carter (Eds), *Cisplatin Current Status and New Developments*. Academic Press, New York (1980) and references therein.
[4] S. J. Lippard (Ed.), *Platinum, Gold and Other Metal Chemotherapeutic Agents*. American Chemical Society, Washington (1983) and references therein.
[5] C. M. Riley, *J. Pharm. Biomed. Anal.* **6**, 669 (1988).
[6] R. Weller, C. M. Riley and L. A. Sternson, *Proc. of the 32nd Annual Conference on Mass Spectrometry and Allied Topics*, p. 707. San Antonio, CA (1984).
[7] R. R. Weller, J. R. Eyler and C. M. Riley, *J. Pharm. Biomed. Anal.* **3(1)**, 87 (1985).
[8] H. R. Schulten, *Int. J. Mass Spectrom. Ion Phys.* **32**, 97 (1979).
[9] J. W. Cowens, L. Pendyala, B. Paul, J. Alderfer, S. Dutta, G. Chheda and P. J. Creaven, *Proc. of the 32nd Annual Conference on Mass Spectrometry and Allied Topics*, p. 711. San Antonio, CA (1984).
[10] J. W. Cowens, F. A. Stevie, J. L. Alderfer, G. E. Hansen, L. Pendyala and P. J. Creaven, *Int. J. Mass Spectrom. Ion Phys.* **48**, 177 (1983).
[11] P. Haake and S. H. Mastin, *J. Am. Chem. Soc.* **93**, 6823 (1971).
[12] D. Dalietos, A. Furst, D. Theodoropoulos and T. D. Lee, *Int. J. Mass Spectrom. Ion Proc.* **61**, 141 (1984).

[13] M. M. Seigel, P. Bitha, R. G. Child, J. J. Hlavka, Y. Lin and T. T. Chang, *Biomed. Environm. Mass Spectrom.* **13**, 25 (1986).
[14] J. Claereboudt, B. De Spiegeleer, C. Lippert, E. A. de Bruijn and M. Claeys, *Proc. International Symposium on Mass Spectrometry of Large Molecules*, Lausanne, Switzerland; *Spectros. Int. J.* **7**, 91 (1989).
[15] H. Vogt, H. J. Heinen, S. Meier and R. Wechsung, *Fres. Z. Anal. Chem.* **308**, 195 (1981).
[16] L. Van Vaeck, J. Claereboudt, P. Van Espen, F. Adams, R. Gijbels and W. Cautreels, *Adv. Mass Spectrom.* **9B**, 957 (1985).
[17] S. C. Dhara, *Ind. J. Chem.* **8**, 193 (1970).
[18] S. Meischen, G. Gale, L. Lake, C. Frangakis, M. Rosenblum, E. Walker, L. Atkins and A. Smith, *J. Natl. Cancer Inst.* **57**, 841 (1976).
[19] B. M. J. De Spiegeleer, P. H. M. De Moerloose and G. A. S. Slegers, *Analyt. Chem.* **59**, 62 (1987).
[20] L. Van Vaeck, J. Claereboudt, J. De Waele, E. Esmans and R. Gijbels, *Analyt. Chem.* **57**, 2944 (1985).
[21] L. Van Vaeck, J. Claereboudt, E. Veldeman, M. Vermeulen and R. Gijbels, *Bull. Soc. Chim. Belg.* **95**, 351 (1986).

[*Received for review 16 May 1989; revised manuscript received 2 June 1989*]